Using Triaxiality Dependent Cohesive Zone Model in Low Cycle Fatigue

Xuan Cao[1,*], Michael Vormwald[1]

[1] Material Mechanics Group, Technische Universität Darmstadt, 64287 Darmstadt, Germany
* Corresponding author: cao@wm.tu-darmstadt.de

Abstract: Cohesive zone models (CZM) are widely used for material fracture analysis. In monotonic loading process, the cohesive parameters are remarkably dependent on the specimens' triaxiality conditions. A cyclic CZM is now introduced for crack initiation life and fatigue crack growth analysis. These two types of fatigue phenomena - crack initiation and fatigue crack growth - are to be described by the cyclic CZM with a unique set of parameters. Fatigue crack initiation is usually investigated using smooth specimen and fatigue crack growth is measured using compact tension specimen. The triaxiality condition in the CZM of these two standard specimens is strongly different. Realistic modelling of the phenomena therefore requires taking the triaxiality into account in the damage evolution law of the cyclic CZM. As a consequence in this paper a cyclic CZM combined with triaxiality dependent characteristic is proposed. This new model can be applied for specimens with different triaxiality conditions. The computation results including crack initiation life and fatigue crack growth simulation are compared with experimental data. In the very low cycle fatigue regime, a reasonable accordance of experimental and calculated results is achieved.

Keywords: Cohesive zone model, Triaxiality dependence, Low cycle fatigue, Damage evolution

1. Introduction

In actual engineering, fracture of the materials and structures is a very dangerous failure form and usually causes serious consequence. Thus, research on mechanisms of material fracture, controlling and reducing occurrence of fracture accidents are always important issues. Fracture mechanics provides the theoretical basis and application approaches for material fracture research. But sometimes the modelling expenses are very high for fracture mechanics concepts and other ideas should be introduced. Among all these methods, the cohesive zone model is very attractive for researchers.

Cohesive zone model (CZM) is an interface damage model, it simplifies the fracture process zone into a narrow cohesive strip. Originally, the concept of CZM has been proposed by Dugdale [1] and Barenblatt [2]. In 1976, the CZM was firstly used by Hillerborg [3] in finite element calculation for concrete material. From then on, the CZM was applied widely as a numerical simulation model for material fracture. In the last 30 years, the CZM was developed by many investigators and scientific groups [4-10]. Now, it becomes a universal tool for material fracture analysis. Especially for material fracture under monotonic loading, the applications of the CZM are successful.

However, using the CZM in material fatigue fracture is still at a starting stage. In the late 1990's, the CZM was firstly extended by De-Andrés et al. [11] for fatigue crack growth simulation. A damage parameter was introduced to indicate the irreversible damage process. But in this model no description about the damage evolution is supplied. Soon afterwards, Yang et al. [12] developed a damage locus in the CZM to simulate fatigue crack growth. However, in this model the unloading and reloading stiffness have different definitions and the damage evolution is just dependent on the damage locus, these treatments are not convenient and accurate for application. Then the cyclic CZM proposed by Roe and Siegmund [13] explicitly introduced a damage variable and a damage evolution equation. The stiffness and traction of the cohesive zone degraded with the damage variable. The numerical calculation results of this model can reproduce many basic characteristics which are similar to the experimental phenomena in fatigue fracture. Nevertheless, there is no experimental verification for the damage evolution process and the other important factors for CZM

are not considered, such as surrounding continuum element influence, element friction influence and constraint condition influence. Base on Roe and Siegmund's method, some authors did further research work [14-16].

2. Cohesive zone model

2.1. Fundamentals

The CZM intends to describe the real physical fracture process by phenomenological equations. It treats the material separation in the fracture process zone as material damage. Separation is the displacement jump occurring in the cohesive element. In the CZM, the material separation behaviour is described within a constitutive equation relating the cohesive traction T to the material separation δ, called traction separation law (TSL). The TSL represents the material deterioration occurring in the damage zone under the monotonic loading condition. For the shape of the TSL many proposals have been given, but no one can easily decide which is right or wrong. For all TSLs, two parameters are contained: maximum traction T_0 and critical separation δ_0. The area under the TSL represents the cohesive energy Γ_0. If the shape of the TSL is selected, the cohesive parameters should be determined from the correlative experiment. In this paper, the TSL from Scheider et al. is taken as a basis (Equation (1) and Figure 1). More details on application of this CZM can be taken from references [8-9].

$$T(\delta)=T_0 f(\delta)=T_0\begin{cases}2\left(\dfrac{\delta}{\delta_1}\right)-\left(\dfrac{\delta}{\delta_1}\right)^2 & \delta<\delta_1\\ 1 & \delta_1\le\delta\le\delta_2\\ 2\left(\dfrac{\delta-\delta_2}{\delta_0-\delta_2}\right)^3-3\left(\dfrac{\delta-\delta_2}{\delta_0-\delta_2}\right)^2+1 & \delta_2<\delta\le\delta_0\end{cases} \tag{1}$$

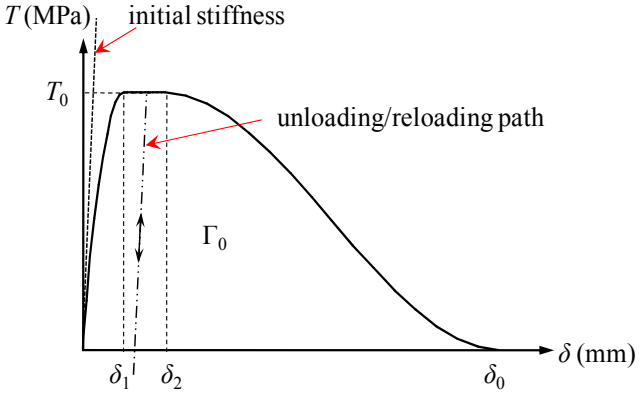

Figure 1. Traction separation law according to Scheider et al. [8], given by Equation (1)

2.2. Triaxiality dependent behaviour

When the phenomenological TSL is applied for ductile fracture analysis, it is possible to find a fundamental relationship between this TSL and micromechanics. A micromechanical model - GTN model [17] is used to simulate a biaxial tension test for one volume element, a cohesion-decohesion curve can be obtained. Such cohesion-decohesion curve is considered as the micromechanical TSL and can be used to fit the phenomenological TSL. For this micromechanical traction separation curve, some investigators found that it was strongly dependent on the triaxiality condition of the

element. Here, the triaxiality value means the ratio between the hydrostatic stress and the von Mises equivalent stress, see Equation (2).

$$H = \frac{\sigma_h}{\sigma_{Mises}} \tag{2}$$

H is the triaxiality value for unit volume element. σ_h is the hydrostatic stress in the element. σ_{Mises} is the von Mises equivalent stress in the element.

The conclusions for triaxiality dependent behavior can be summarized as: the cohesive parameters are not pure material constants but dependent on the triaxiality conditions. With increasing the triaxiality value, the material maximum traction T_0 becomes bigger but the material critical separation δ_0 and cohesive energy Γ_0 become smaller. Details about this investigation can be consulted in references [18-20]. When the triaxiality dependent behaviour is implemented into the CZM, the triaxiality value can only be obtained from the surrounding continuum element and has to be transferred to the cohesive element.

3. Extended CZM for fatigue fracture

3.1. Overview

The ordinary TSLs just describe the material fracture failure under monotonic loading condition. For material fatigue fracture properties, other approaches need to be introduced. By reviewing some ideas from pioneers, a tentative method of Roe and Siegmund [13] is chosen as starting point. Considering the theory of continuum damage mechanics, a damage variable and a corresponding damage evolution law are introduced in the CZM following ideas of Scheider [8]. This cyclic CZM is used for fatigue fracture analysis.

In respect to the fatigue fracture process, the important research topics focus on fatigue crack initiation life and fatigue crack growth rates analysis. In experimental investigation, fatigue crack initiation is usually tested using uncracked smooth specimen and fatigue crack growth is measured using pre-cracked specimen. The triaxiality conditions for these two standard specimens are totally different. When the CZM is applied for simulation of these two fatigue phenomena, it is necessary to take the triaxiality influence into account in the damage process.

So, a triaxiality dependent cyclic CZM is now proposed. The model should be implemented to reproduce fatigue experimental phenomena which contain fatigue crack initiation and fatigue crack growth, just using a unique set of parameters. For simplicity, in this paper just mode-I fracture is considered. This means in the CZM just normal separation contributes to the damage.

3.2. Fatigue damage process

With the damage variable D, the cohesive strength and normal stiffness of the cohesive element will degrade (Equation (3) and Equation (4)).

$$T_0^N = \left[T_{0\,(H)}^N \right] (1 - D) \tag{3}$$

$$k_N = k_N (1 - D) = \frac{2T_0^N}{\delta_1} \tag{4}$$

T_0^N and $\overline{T}_0^N$ are the initial and current normal cohesive strength, the subscript (*H*) represents that the initial cohesive strength is dependent on the triaxiality condition. k_N and $\overline{k}_N^0$ are the initial and current normal stiffness of the cohesive element. δ_1 is a parameter relating to the critical separation δ_0, the meaning is the same as in Equation (1).

For the triaxiality dependent cyclic CZM, it is difficult to judge the loading and unloading conditions because the separation δ and the critical separation δ_0 of the cohesive element alter simultaneously. So, a relative normal separation and its increment are defined by Equation (5) and Equation (6):

$$\delta_{re}^N = \frac{\delta^N}{\delta_{0\,(H)}^N} \tag{5}$$

$$\Delta\delta_{re}^N = \frac{\delta_t^N}{\delta_{0\,(H_t)}^N} - \frac{\delta_{t-\Delta t}^N}{\delta_{0\,(H_{t-\Delta t})}^N} = \delta_{re\,(t)}^N - \delta_{re\,(t-\Delta t)}^N \tag{6}$$

δ_{re}^N and δ^N are the relative and absolute normal separation, respectively. δ_0^N is the critical normal separation, the subscript (*H*) represents that it is dependent on the triaxiality condition. $\Delta\delta_{re}^N$ is the relative normal separation increment. The subscripts *t-Δt* and *t* stand for the previous and current calculation time increment. $\delta_{t-\Delta t}^N$ and δ_t^N, $\delta_{0\,(H_{t-\Delta t})}^N$ and $\delta_{0\,(H_t)}^N$, $\delta_{re\,(t-\Delta t)}^N$ and $\delta_{re\,(t)}^N$ correspond to the absolute normal separation, the critical normal separation and the relative normal separation in the time increment *t-Δt* and *t*, respectively. If in the different time increment the triaxiality condition does not change, the two critical separations $\delta_{0\,(H_{t-\Delta t})}^N$ and $\delta_{0\,(H_t)}^N$ should be the same.

A loading step is indicated by $\Delta\delta_{re}^N > 0$, an unloading step is indicated by $\Delta\delta_{re}^N < 0$. At the first loading step, the traction separation response goes along the monotonic TSL's path (Equation (1)). Afterwards the unloading and reloading process is defined by Equation (7).

$$T_t^N = T_{t-\Delta t}^N + \overline{k}_N^0 \left[\Delta\delta_{re}^N * \delta_{0\,(H_t)}^N \right] \tag{7}$$

$T_{t-\Delta t}^N$ and T_t^N are the normal traction in the time increment *t-Δt* and *t*. The meanings for the other symbols can be checked in the previous paragraphs.

In every loading process a maximum relative normal separation $\delta_{re\,\max}^N$ may be reached. During the reloading process, when the current relative normal separation exceeds this maximum value, Equation (8) is used for the new path.

$$T^N = \begin{cases} \overline{T}_0^N \left[2\left(\dfrac{\delta^N}{\delta_1}\right) - \left(\dfrac{\delta^N}{\delta_1}\right)^2 \right] & \delta_{re}^N \le \dfrac{\delta_1}{\delta_{0\,(H)}^N} \\ \overline{T}_0^N & \delta_{re}^N > \dfrac{\delta_1}{\delta_{0\,(H)}^N} \end{cases} \tag{8}$$

In the unloading process, it is still an open topic how the triaxiality influences the cohesive parameters. In this paper, a simple assumption is made. The triaxiality value keeps constant in the unloading process and a part of the reloading process. The definition about this part of the reloading

process is like Equation (8). When the current relative normal separation is less than δ_{re}^{N}, the triaxiality value keeps constant. Once δ_{re}^{N} is exceeded, the triaxiality value updates again.

After the cohesive element is broken, in the unloading or compression period in order to avoid the adjacent continuum element penetrating each other, a contact condition should be considered. Here, when δ^{N} <0, Equation (9) is used.

$$T^{N} = k_{N}\delta^{N} \tag{9}$$

A new damage evolution equation is proposed here, as Equation (10)

$$\dot{D} = \left(\frac{A^{\frac{1}{H}} e^{(\lambda - H)}}{H}\right) \Delta\delta_{re}^{N} \left[\frac{T^{N}}{\left[T_{0}^{N}{}_{(H)}\right](1-D)} - \frac{\sigma_{e}}{T_{0}^{N}{}_{(H)}}\right]^{m} \qquad \dot{D} \geq 0 \tag{10}$$

D is the damage variable. $\dot{D}$ is the damage evolution. It is always a positive value. $T_{0}^{N}{}_{(H)}$ is the triaxiality dependent normal cohesive strength. T^{N} is the cohesive traction. $\Delta\delta_{re}^{N}$ is the relative normal separation increment. σ_{e} is the material endurance limit. H is the triaxiality value. A and m are the material dependent damage controlling parameters. λ is the material dependent triaxiality influence coefficient.

A schematic illustration for the cyclic process of the CZM is shown in Figure 2. The new cyclic CZM is contained in a user defined subroutine, and it is connected with the commercial finite element program ABAQUS. The fatigue damage is calculated for every time increment.

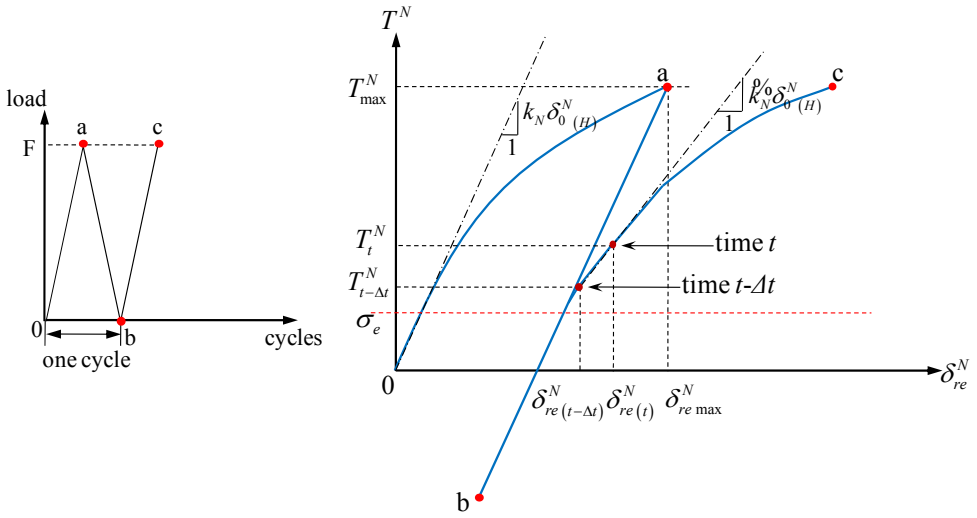

Figure 2. Schematic illustration for cyclic process of the CZM

4. Numerical application

The triaxiality dependent cyclic CZM is applied for fatigue simulation. For triaxiality dependent behavior, some results from literature [20] are used. In reference [20], the examined material is S460N. For convenience, material S460N is chosen for the whole investigations in this paper, too. Some basic mechanical properties for material S460N are shown in Table 1.

Table 1. Mechanical properties for material S460N

Material	E(MPa)	σ_Y(MPa)	R_m(MPa)	K'	n'	σ_e(MPa)
S460N	208000	470	682	1181	0.161	312

E is the material Young's modulus. σ_Y is the material yield stress. R_m is the material ultimate tensile strength. K' is the material cyclic hardening coefficient. n' is the material cyclic hardening exponent. σ_e is the material endurance limit.

4.1. Damage parameters analysis

For the chosen material, the unknown damage parameters in the damage evolution law are just A, m and λ. The material dependent triaxiality influence coefficient λ is fixed first for λ=1.2. The decision for this parameter is based on many trial calculations and a little supposition. The recommendation λ value for material S460N ranges between 0.8 and 1.2, a change of the parameter λ will influence the other two parameters A and m. After λ is chosen, a simple simulation is applied to analyze the material dependent damage controlling parameters A and m. The finite element model consists of two plane strain elements (CPE4) connected by one cohesive element. The model is loaded by cyclic displacement, the loading ratio is R=-1.

In order to reflect the real material response under cyclic loading, the material behavior for continuum element uses a nonlinear kinematic hardening model in ABAQUS. Three different ways are offered by ABAQUS to define the nonlinear kinematic hardening component, specifying the material parameters directly, specifying half-cycle test data or specifying test data from a stabilized cycle. In this paper, nonlinear kinematic hardening model is identified from the stabilized cyclic test. Series of the parameters A and m are investigated and the calculation results are plotted in the material strain-life curve, shown in Figure 3.

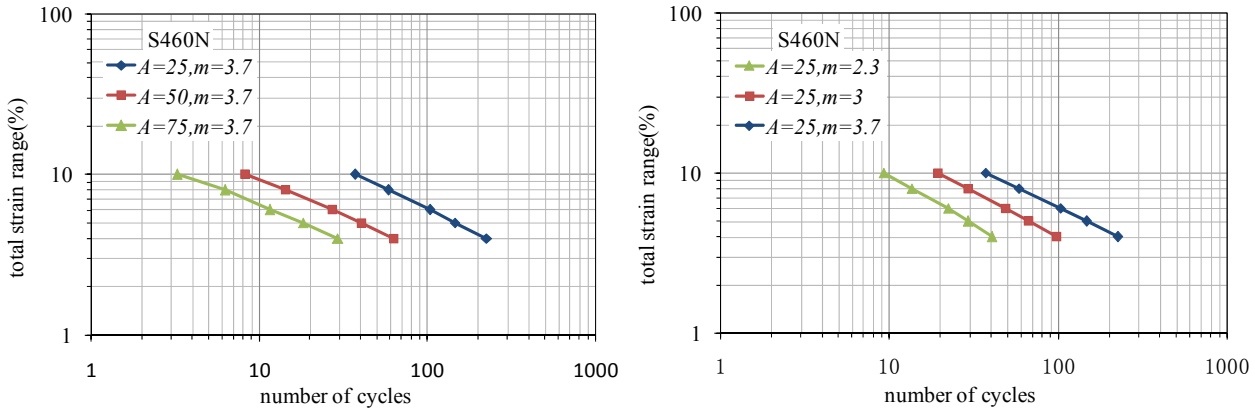

Figure 3. Effect of damage controlling parameters A and m

It is obvious that the parameter m influences the slope of the strain life curve. With increasing the value of m, the slope of the strain-life curve becomes flatter. The parameter A does not influence the slope of the strain-life curve. However, it makes the curve moving parallelly. According to these rules, the parameters A and m can be identified by fitting the numerical results to the experimental strain-life curve.

4.2. Fatigue crack initiation simulation

The strain-life curve of the material S460N is expressed by Equation (11)

$$\varepsilon_a = \varepsilon_{a,el} + \varepsilon_{a,pl} = \frac{\sigma_f'}{E}(2N)^b + \varepsilon_f'(2N)^c \tag{11}$$

ε_a is the strain amplitude. $\varepsilon_{a,el}$ and $\varepsilon_{a,pl}$ are the elastic and plastic part for the strain amplitude. E is the Young's modulus. N is the fatigue life, it stands for fatigue crack initiation life or fatigue fracture life. Here it means the fatigue crack initiation life. σ_f' is the fatigue strength coefficient. b is the fatigue strength exponent. ε_f' is the fatigue ductility coefficient. c is the fatigue ductility exponent. Values are taken from reference [21] and shown in Table 2.

Table 2. Experimental strain-life curve parameters

Material	E(MPa)	σ_f'(MPa)	ε_f'	b	c
S460N	208000	1218	0.452	-0.104	-0.536

In the previous section, the influence rules of the damage controlling parameters A and m are discussed. By fitting the simulation results to the experimental strain-life curve, the parameters A and m can be determined. Here the simulation model is also two plane strain elements connected by one cohesive element. The loading condition and the material behaviour are like in the previous section. The investigations just focus on the very low cycle fatigue regime, so the calculated number of cycles is within 600. For material S460N, the parameters A and m are fitted as: A=25, m=3.7. The experiment and simulation results are plotted in Figure 4.

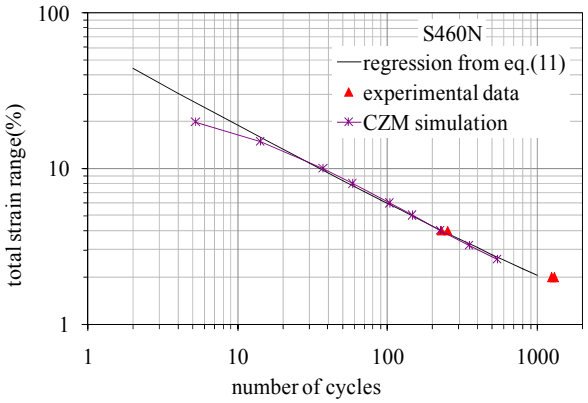

Figure 4. Comparison of strain-life curve for material S460N

4.3. Fatigue crack propagation simulation

For the material S460N, the damage parameters are determined: λ=1.2, A=25 and m=3.7. These parameters need further validation. As an important part of fatigue fracture, the fatigue crack growth simulation is applied here to validate the damage parameters.

The experimental data of fatigue crack growth for the material S460N are taken from reference [22]. The experimental fatigue crack growth rate curve includes four different strain range levels, i.e. $\Delta\varepsilon$=0.4%, $\Delta\varepsilon$=0.6%, $\Delta\varepsilon$=1.0% and $\Delta\varepsilon$=2.0%. Because the investigations focus on very low cycle fatigue regime, just the experimental data at fast crack growth rate are used for comparison.

The numerical model is a two dimensional compact tension specimen. The dimension of the model is width 50mm and height 60mm. The initial crack length a_0 is 25mm and the ligament length is 25mm, too. The type of the continuum element is plane strain. The material behaviour of the continuum elements is the same as in the previous section. The cohesive elements locate along the

ligament and the size of the element is 0.125mm. The details for the finite element model are depicted in Figure 5.

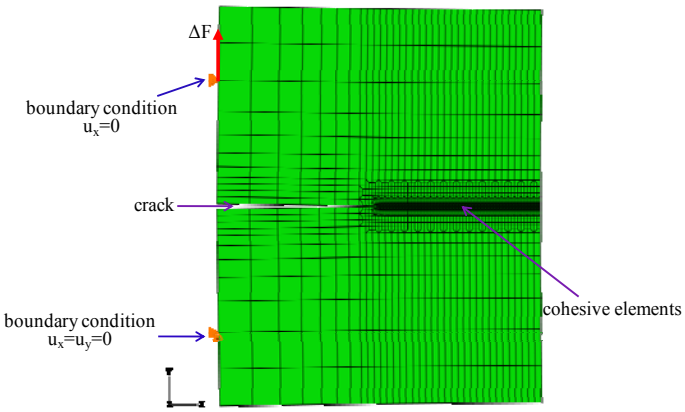

Figure 5. Finite element model for simulated compact tension specimen

In the calculation, three different cyclic loading ranges are used: ΔF=1200N, ΔF=950N and ΔF=800N. All loading ratios are R=0. The fatigue crack growth rate $\Delta a/\Delta N$ can be calculated directly from the numerical model, but the cyclic ΔJ integral will be computed by another approach. A finite element model of the CT specimen without cohesive zone is built. The crack length inserted in this model is $(a_0+\Delta a)$. One cycle is calculated and the cyclic ΔJ integral is computed by Equation (12) [23].

$$\Delta J = \int_{\Gamma}\left(\Delta W dy - \Delta t_i \frac{\partial \Delta u_i}{\partial x} ds\right) \qquad \Delta W = \int_0^{\Delta\varepsilon} \Delta\sigma_{ij} d\Delta\varepsilon_{ij} \tag{12}$$

$\Delta\sigma_{ij}$ and $\Delta\varepsilon_{ij}$ are the cyclic stress and strain range. W is the cyclic deformation energy. x and y are the Cartesian coordinates with the x-axis parallel to the crack surface. Γ is the integration path. ds is the line element lying on the integration path. Δt_i is the cyclic stress vector on the integration path. Δu_i is the cyclic displacement variation.

The simulation results under three loading ranges are plotted together with the scatter band of experimental data in Figure 6.

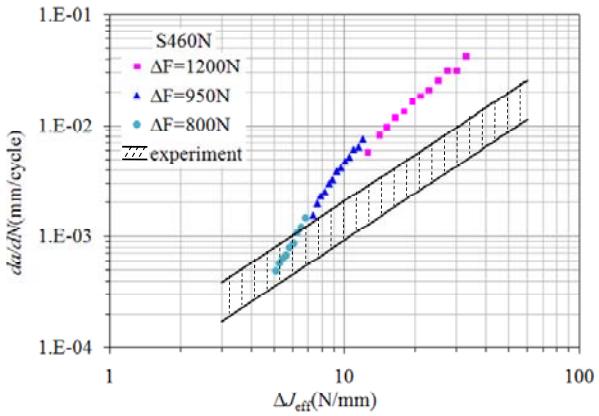

Figure 6. Comparison of fatigue crack growth rates curve for material S460N

A reasonable accordance of experimental and simulated results is achieved. The simulated fatigue crack growth rates are a little bit faster than the experimental data, but the total trend for fatigue

crack growth is very similar. One possible reason for this diversity is from the influence of the model dimension. In experiment, the specimen is a three dimensional model, but in simulation a two dimensional model is used. The calculation about the energy integral ΔJ is bigger for two dimensional problems than for three dimensional problems. The other possible reason is from the new CZM. This numerical model may express the real cyclic process inaccurately.

5. Conclusions

CZM is a very robust numerical tool for material fracture analysis. It is simple enough for theoretical understanding and practical application. For the material monotonic fracture, the implementation of the CZM is particularly mature. But for fatigue fracture analysis, the application is just in developing. In this paper, according to the pioneers' idea [13], a triaxiality dependent cyclic CZM is proposed. This model can be applied for various triaxiality conditions, and only one set of unique material damage parameters is used. In the very low cycle fatigue regime, using the triaxiality dependent cyclic CZM in fatigue crack initiation and fatigue crack growth simulation, the reasonable comparison results between experiment and simulation can be obtained.

However, this new CZM is still in a testing process. Many improvements and developments need to be done in the future. More materials should be chosen in the simulation to validate the new CZM. The cyclic process for the CZM needs more discussions, especially in unloading and compression period. The format of the damage evolution law maybe modified. The triaxiality dependent behavior in the whole cyclic process needs much more investigations.

Acknowledgements

Author would like to thank Dr. Ingo Scheider from Helmholtz-Zentrum Geesthacht, Institut für Werkstoffforschung, for providing many helpful suggestions in cohesive zone model application.

References

[1] D.S. Dugdale, Yielding of steel sheets containing slits. Journal of the Mechanics and Physics of Solids, 8 (1960) 100-104.
[2] G.I. Barenblatt, The mathematical theory of equilibrium cracks in brittle fracture. Advances in Applied Mechanics, 7 (1962) 55-129.
[3] A. Hillerborg, M. Modéer, P.E. Petersson, Analysis of crack formation and crack growth in concrete by means of fracture mechanics and finite elements. Cement and Concrete Research, 6 (1976) 773-782.
[4] A. Needleman, A continuum model for void nucleation by inclusion debonding. Journal of Applied Mechanics, 54 (1987) 525-531.
[5] A. Needleman, An analysis of decohesion along an imperfect interface. International Journal of Fracture, 42 (1990) 21-40.
[6] V. Tvergaard, J.W. Hutchinson, The relation between crack growth resistance and fracture process parameters in elastic-plastic solids. Journal of the Mechanics and Physics of Solids, 40 (1992) 1377-1397.
[7] H. Yuan, G.Y. Lin, A. Cornec, Verification of a cohesive zone model for ductile fracture. Journal of Engineering Materials and Technology, 118 (1996) 192-200.
[8] A. Cornec, I. Scheider, K.H. Schwalbe, On the practical application of the cohesive model. Engineering Fracture Mechanics, 70 (2003) 1963-1987.
[9] I. Scheider, W. Brocks, Simulation of cup-cone fracture using the cohesive zone model. Engineering Fracture Mechanics, 70 (2003) 1943-1961.

[10] N. Chandra, H. Li, C. Shet, H. Ghonem, Some issues in the application of cohesive zone models for metal-ceramic interfaces. International Journal of Solids and Structures, 39 (2002) 2827-2855.
[11] A. De-Andrés, J.L. Pérez, M. Ortiz, Elastoplastic finite element analysis of three-dimensional fatigue crack growth in aluminium shafts subjected to axial loading. International Journal of Solids and Structures, 36 (1999) 2231-2258.
[12] B. Yang, S. Mall, K. Ravi-Chandar, A cohesive zone model for fatigue crack growth in quasibrittle materials. International Journal of Solids and Structures, 38 (2001) 3927-3944.
[13] K.L. Roe, T. Siegmund, An irreversible cohesive zone model for interface fatigue crack growth simulation. Engineering Fracture Mechanics, 70 (2003) 209-232.
[14] A. Abdul-Baqi, P.J.G. Schreurs, M.G.D. Geers, Fatigue damage modeling in solder interconnects using a cohesive zone approach. International Journal of Solids and Structures, 42 (2005) 927-942.
[15] J.L. Bouvard, J.L. Chaboche, F. Feyel, F. Gallerneau, A cohesive zone model for fatigue and creep-fatigue crack growth in single crystal superalloys. International Journal of Fatigue, 31 (2009) 868-879.
[16] Y.J. Xu, H. Yuan, On damage accumulations in the cyclic cohesive zone model for XFEM analysis of mixed-mode fatigue crack growth. Computational Materials Science, 46 (2009) 579-585.
[17] P. Nègre, D. Steglich, W. Brocks, Crack extension in aluminium welds: a numerical approach using the Gurson-Tvergaard-Needleman model. Engineering Fracture Mechanics, 71 (2004) 2365-2383.
[18] T. Siegmund, W. Brocks, The role of cohesive strength and separation energy for modeling of ductile fracture. Fatigue and Fracture Mechanics, 30 (2000) 139-151.
[19] M. Anvari, I. Scheider, C. Thaulow, Simulation of dynamic ductile crack growth using strain-rate and triaxiality-dependent cohesive elements. Engineering Fracture Mechanics, 73 (2006) 2210-2228.
[20] I. Scheider, Derivation of separation laws for cohesive models in the course of ductile fracture. Engineering Fracture Mechanics, 76 (2009) 1450-1459.
[21] CHR. Boller, T. Seeger, Materials data for cyclic loading-part B: low-alloy steels, Elsevier Science Publishers B.V., Amsterdam, 1987.
[22] M. Vormwald, Ermüdungslebensdauer von Baustahl unter komplexen Beanspruchungsabläufen am Beispiel des Stahles S460. Materials Testing, 53 (2011) 98-108.
[23] C. Wüthrich, The extension of the J-integral concept to fatigue cracks. International Journal of Fracture, 20 (1982) 35-37.